The relationship of lightning radio pulse amplitudes and source altitudes as observed by LOFAR

J. G. O. Machado [1], B. M. Hare [2], O. Scholten [2,3], S. Buitink [4,5], A. Corstanje [4,5], H. Falcke [4,6,7], J.R. Hörandel [4,5,6], T. Huege [5,8], G. K. Krampah [5], P. Mitra [5], K. Mulrey [5], A. Nelles [9,10], H. Pandya [5], J. P. Rachen [5], S. Thoudam [11], T. N. G. Trinh [12], S. ter Veen [4,7], T. Winchen [13]

[1]Physics Institute, University of Brasilia, Brasilia, DF 70910-900, Brazil

[2] Kapteyn Astronomical Institute, University of Groningen, P.O. Box 72, 9700 AB Groningen, Netherlands

[3] Interuniversity Institute for High-Energy, Vrije Universiteit Brussel, Pleinlaan 2, 1050 Brussels, Belgium

[3]Department of Physics and Astronomy, University of New Hampshire, Durham, NH, USA

[4]Department of Astrophysics/IMAPP, Radboud University Nijmegen, P.O. Box 9010, 6500 GL Nijmegen, Netherlands

[5]Astrophysical Institute, Vrije Universiteit Brussel, Pleinlaan 2, 1050 Brussels, Belgium

[6]NIKHEF, Science Park Amsterdam, 1098 XG Amsterdam, Netherlands

[7]Netherlands Institute of Radio Astronomy (ASTRON), Postbus 2, 7990 AA Dwingeloo, Netherlands

[8]Institute for Astroparticle Physics (IAP), Karlsruhe Institute of Technology (KIT), P.O. Box 3640, 76021, Karlsruhe, Germany

[9] DESY, Platanenallee 6, 15738 Zeuthen, Germany

[10] ECAP, Friedrich-Alexander-University Erlangen-Nürnberg, 91058 Erlangen, Germany

[11]Department of Physics, Khalifa University, PO Box 127788, Abu Dhabi, United Arab Emirates

[12]Department of Physics, School of Education, Can Tho University Campus II, 3/2 Street, Ninh Kieu District, Can Tho City, Vietnam

[13]Max-Planck-Institut für Radioastronomie, P.O. Box 20 24, Bonn Germany

Key Points:

- We measure the amplitude distribution of lightning VHF pulses
- The VHF pulse amplitude spectrum follows a power-law
- The top 10-percentile amplitude decreases with altitude

Corresponding author: João Machado, j04ogm@gmail.com

Abstract

When a lightning flash is propagating in the atmosphere it is known that especially the negative leaders emit a large number of Very High Frequency (VHF) radio pulses. It is thought that this is due to streamer activity at the tip of the growing negative leader. In this work we have investigated the dependence of the strength of this VHF emission on the altitude of the negative leader as observed by the LOFAR radio telescope. We find that the extracted amplitude distributions are consistent with a power-law, and that the amplitude of the radio emissions decreases very strongly with source altitude, by about a factor of 2 from 1 km altitude up to 5 km altitude. In addition, we do not find any dependence on the extracted power-law with altitude, and that the extracted power-law slope has an average around 3.

1 Introduction

It is thought that VHF (30-300 MHz) radio emission from lightning is dominated by streamer activity (Shi et al., 2019; Hare et al., 2020). From laboratory experiments (Nijdam et al., 2020; Li et al., 2016) it is known that the streamer activity depends strongly on air density. In particular (T.M.P et al., 2008; T et al., 2013) have shown that streamer propagation speed increases with decreasing air density. Therefore, in one model it is natural to expect that the amplitude of VHF radio emission from lightning should vary with pressure. Since streamers can be thought of as a moving head of charge, the VHF emission should be roughly proportional to the charge of the streamer times its acceleration. Since the velocity of a streamer increases with decreasing density, the acceleration should increase as well, thus it may be reasonable to expect that the VHF emission from lightning should increase at higher altitudes. However, alternatively, in the laboratory experiments of (Li et al., 2016) have shown that the amplitude of the corona current pulse decreases less than linear with decreasing air pressure, while the width of the current pulse increases much stronger than linear when keeping the same ratio between applied voltage and onset voltage [fig 6, (Li et al., 2016)]. This thus implies that that the time-derivative of the corona current, and thus the VHF emission, should strongly decrease with altitude, in stark contrast to the previous model.

It is thus of much interest to investigate the density (or equivalently the altitude) dependence of VHF emission from streamers. This is indicative of the basic physics behind the lightning corona, although the detailed relationship is not understood. Following the work of (Hare et al., 2020, 2019; Scholten et al., 2021), we have investigated the VHF emission from negative lightning leaders using the LOFAR radio telescope over the altitude range from 0 up to 6 km where the pressure at 6 km is roughly half the pressure at ground level. We have found that over this range, the emitted VHF decreases by about a factor of three.

In section 2 we describe how the data and how it was analysed. The obtained results are given in section 3, and in section4 this data is interpreted and compared with laboratory results from other studies.

2 Methods

We investigated two lightning flashes, one from 29 September 2017 at 17:34:55 UTC, and another from 13 August 2018 at 15:30:01 UTC, referred to as the "2017" and "2018" flashes respectively, that were detected by LOFAR and imaged as described in section 2.1. In order to investigate the effect of pressure on the VHF emission of lightning, we selected negative leaders from these two flashes and found the distribution of recorded pulse peak amplitudes at different altitudes with 500 m tall altitude bins. For the VHF-sources located on negative leaders within a certain altitude range we determined the

spectrum of peak amplitudes in a reference antenna. These spectra are analyzed in section 2.2.

2.1 Lightning Imaging and the LOFAR Radio Telescope

The LOFAR (Low Frequency ARray) is a high precision radio telescope capable of locating lightning VHF sources with meter and nanosecond precision. It consists of over 4512 low-band antennas and 2256 high-band antennas distributed within dozens of stations scattered across The northern Netherlands. There are also international stations in other European countries, but they are not used for mapping lightning. For lightning observations we use the The low-band antennas operating over the $10 \sim 90$ MHz range(van Haarlem et al., 2013).

During processing, RFI lines due to radio stations are filtered-out, and each of these flashes used in this work was imaged using a Kalman-filter-inspired imaging algorithm (Scholten et al., 2021), which locates the source region of recorded radio pulses with meter scale accuracy. Figure 1 shows the image of the 2017 flash, with the negative leaders used in this work indicated.

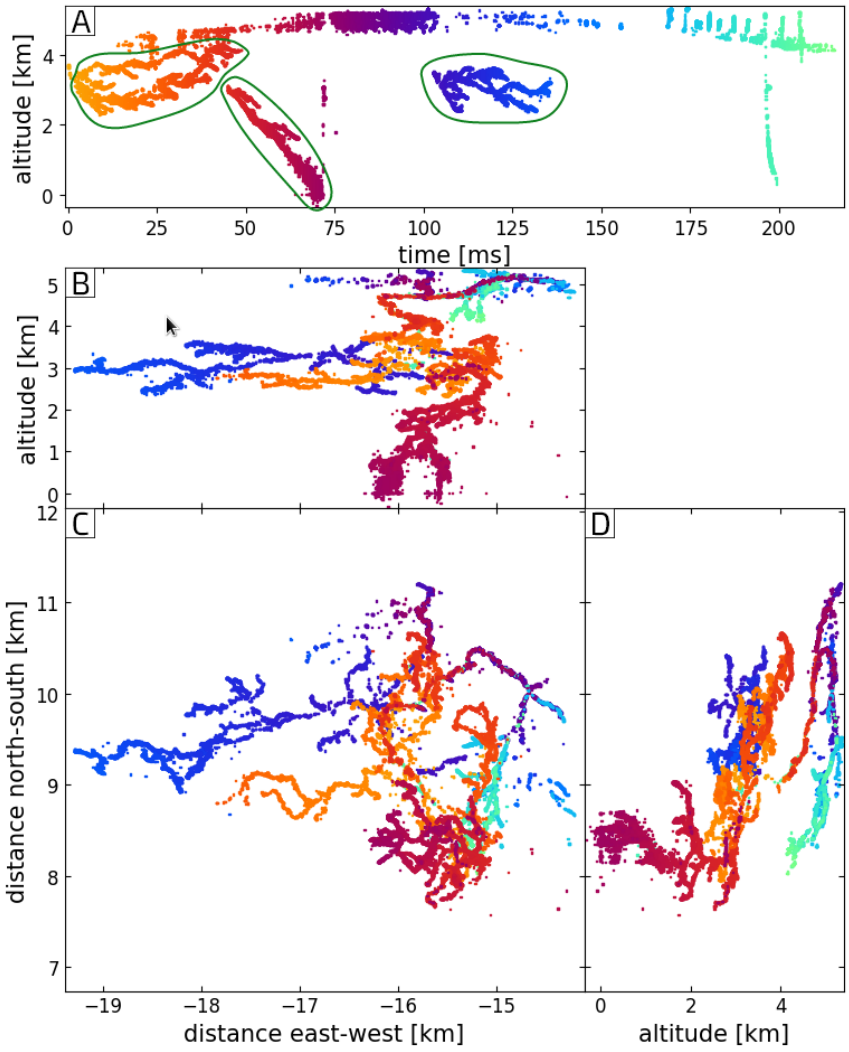

Figure 1. Plan view of the imaged data, coloured by time. Each point represents a located VHF source. Negative leaders are circled in green. A) Time vs altitude (from ground). B) east-west distance (from core center) vs altitude. C) east-west distance (from core center) vs north-south (from core center). D) altitude (from ground) vs east-west distance (from core center).

2.2 Analysis of Pulse Amplitudes

The radio emission from negative leaders, as observed by LOFAR, is extremely impulsive, where each recorded pulse has a full-width-half-max (FWHM) of around 50 ns. As a proxy for the amplitude of each radio source, the peak amplitude of the pulse is taken as recorded by a central antenna, called the reference antenna. Since we are only interested in how the amplitude changes with source altitude, we have not performed any absolute calibration, (Mulrey et al., 2019), and only present the amplitudes as measured by the digitizer. There are multiple factors that can affect how the measured pulse amplitude relates to the actual VHF-pulse amplitude at the source which will be discussed in a later section. The negative leaders from the two flashes we consider in this work were arranged in 500 m tall altitude bins and for each bin the strength distribution of the sources is analyzed.

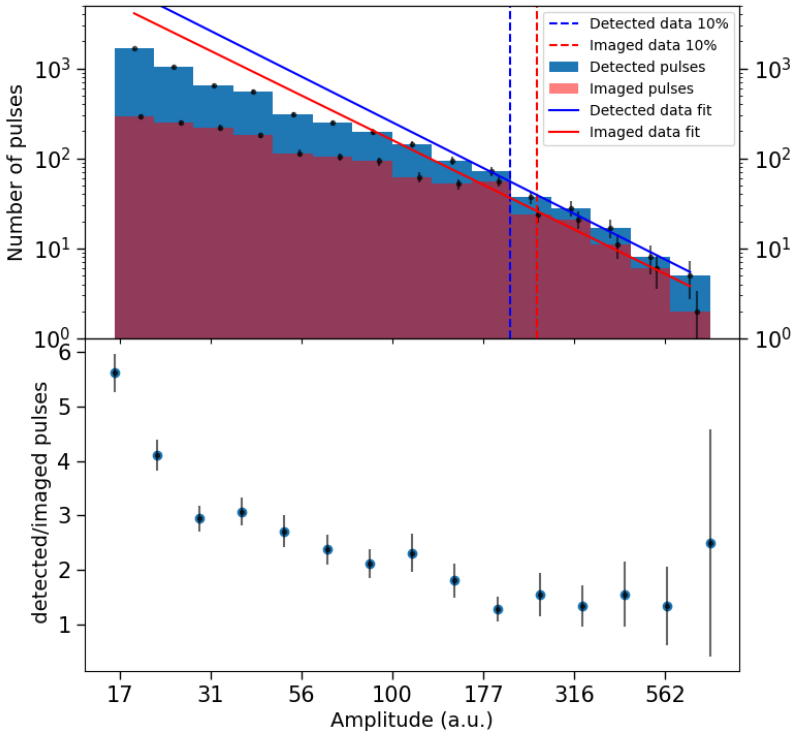

Figure 2. The upper image shows on a log-log scale an overlapping comparison between the distributions of amplitudes of located sources and all pulses as detected in the reference antenna between times $t = 100$ ms and $t = 150$ ms from the 2017 flash. The solid lines show a power-law fit to the strongest 10% of sources, and the vertical bar shows the 10% amplitude. The power-law slope, λ, for both fits is 2.32. The lower panel depicts the ratio of the number of located and all pulses per amplitude bin. Amplitude is in arbitrary units.

The efficiency of our imaging algorithm depends on pulse strength, strong pulses clearly stick out and are thus more easily recognized as the weaker ones. This potentially introduces a pulse-height dependent bias. To explore this, figure 2 shows the amplitude spectrum of all received radio pulses between times $t = 100$ ms and $t = 150$ ms from the 2017 flash shown in figure 1, as well as amplitude spectrum of the located sources in the same time period. We have made this selection because there was very little ac-

tivity elsewhere at this time, and because the negative leaders occurred over a relatively narrow altitude range. For most other cases this comparison cannot be made as there is lightning activity at many different altitudes and it is necessary to locate the source. As expected, the source locations could be found for almost all strong peaks and for the weaker ones the pulse-finding efficiency becomes gradually worse. This is also expressed in the lower panel of figure 2, showing that the ratio between the two amplitude distributions (number of located divided by the number of all pulses) is fairly constant and close to unity for the strongest 10% pulses. This is also shown by the fact that fits to the strongest 10% pulses with a power-law 1, a straight lines on a log-log scale, as described later in this section, yield the same slopes for the two distributions. Therefore we focus in this work on the strongest 10% of located pulses where the 10-percentile amplitude is indicated by the vertical dashed line in the figure.

To characterize the pulse distribution at large amplitudes we explored two different statistics. The absolute pulse strength is characterized by the 10-percentile amplitude. We choose this statistic because the maximum amplitude for a stochastic process will increase with the number of analyzed pulses while a percentile value is more stable. We have opted for the 10% amplitude since this is the largest percentile that is not much affected by the imaging efficiency as seen from figure 2. The two vertical bars in figure 2 show the 10% cut amplitude for the imaged and all pulses. Due to the smaller imaging efficiency at smaller amplitudes the 10% value for all pulses is somewhat smaller than for the imaged sources. However we do not expect this to significantly influence our results as a similar affect should occur at all altitudes. In addition we also report the slope λ of a power-law fitted to the strongest 10% of events,

$$N(a) = N_0 a^{-\lambda} \,, \tag{1}$$

where $N(a)$ is the number of number of events at amplitude a and N_0 is a normalization factor. We have opted for a power-law instead of an exponential distribution as this yields a better fit to the data.

2.3 Correction Factors

There are several factors that affect the relation between the detected pulse amplitude and the actual emitted amplitude. Some of these will be important for the height dependence we investigate in this work.

Since an impulsive source is likely driven by a rapidly changing current with a certain orientation, the VHF emission will have an angle-dependent emission pattern, likely similar to dipole emission. However, since we consider the emission from many sources that are likely to have random orientations, this emission-pattern imprint should average out. Sources that are further away will have weaker recorded amplitudes in the reference antenna. This however, is not a significant concern as the spatial extent of each of the three flashes is much smaller than the distance to the flash itself ($\approx$ 18.6 km for 2017 flash and $\approx$ 50 km for the 2018 flash). Therefore, while our measured amplitudes cannot be compared between flashes, the shape of the amplitude distribution should be robust to distance variations within each lightning flash.

More importantly, however, are the effects of LOFAR's antenna function. Radio emission from different sources will arrive at different elevation (θ_e) and azimuth (ϕ) angles, and therefore be amplified differently by the antenna function. The azimuth-angle dependence is not very strong as all sources are in a small angular regime where the antenna function is large. Particular care needs to be given to the elevation angle as the LOFAR antennas have vanishing sensitivity for sources at $\theta_e = 0$. Basic analytic considerations for the angular dependence of the measured amplitude one thus concludes that the antenna function is proportional to $\sin(\theta_e)$ for the small values of θ_e that are relevant for this work. Since $\sin(\theta_e) \approx \tan(\theta_e) = h/R$, where h is the altitude of the

source and R the distance. One should correct for this linear altitude dependence to deduce the true height dependence of the source amplitude from the measured amplitude.

3 Results

Figure 1 show the results for the extracted statistics on the pulse distributions for the 2017 and 2018 flashes respectively. For each the altitude range, the number of located sources, the 10% percentile amplitude a_{10}^d, the same value corrected for the antenna function a_{10}^c, and the fitted power-law slope. As we have argued in section 2.3 the correction of the pulse strength is inversely proportional to the height of the source. Normalizing the correction to unity at 5 km we thus obtain

$$a_{10}^c = \frac{5}{h} a_{10}^d \,, \tag{2}$$

where h is the mean altitude of the bin in units of km.

Table 1. The parameters for the amplitude distributions for negative leaders at different altitude sections for the two flashes considered in this work. The first column is the altitude range. For each flash the first gives the number of sources in the negative leader at that height, the second column gives the 10-percentile value of the measured amplitude, which is corrected for the effects of the antenna function in the third column, and the last column gives the the power-law slope, λ.

	2017 flash				2018 flash			
Height	sources	a_{10}^d	a_{10}^c	λ	sources	a_{10}^d	a_{10}^c	λ
0.0 - 0.5 km	353	137	2740	3.62	74	99	1980	4.64
0.5 - 1.0 km	1077	215	1433	2.42	110	93	620	2.50
1.0 - 1.5 km	910	255	1020	1.73	368	102	408	2.85
1.5 - 2.0 km	1643	292	834	2.45	721	116	331	4.03
2.0 - 2.5 km	1496	311	691	2.28	893	123	273	4.46
2.5 - 3.0 km	3714	312	567	2.90	1866	137	249	3.42
3.0 - 3.5 km	3110	322	795	2.93	2818	149	229	3.31
3.5 - 4.0 km	1709	324	432	2.11	3434	162	216	3.51
4.0 - 4.5 km	652	286	336	2.65	2048	166	195	2.48
4.5 - 5.0 km					429	200	210	1.82
5.0 - 5.5 km					25	156	148	1.05

4 Discussion and Conclusion

Our data show that the a_{10}^d values tends to increase slowly with altitude, however when corrected for the antenna function, a_{10}^c, the values rapidly decrease with altitude as can be seen from figure 3. The a_{10}^c values for the two flashes almost fall on top of each other if those for 2018 are normalized to each other for the 2 – 2.5 Km altitude bin, suggesting that the observed, approximately exponential, dependence on pressure or height is rather general. Such a re-scaling is reasonable since the 2018 flash is at a larger distance from the reference antenna than the 2017 flash.

The laboratory results as reported in (Li et al., 2016) indicate that, for a fixed value of the electric field over breakdown, the electrical current decreases with decreasing pressure while at the same time also the width of the current pulse increases. Figure 6 of (Li et al., 2016) indicates that the pulse-width increases by about a factor three when the

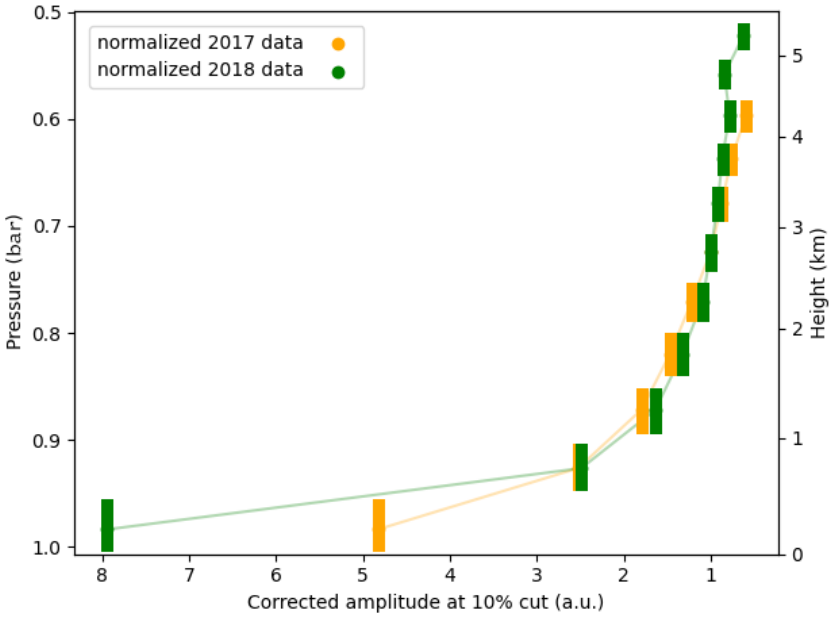

Figure 3. The pressure (left scale) and height (right scale) dependence of the corrected ten-percentile amplitudes (a_{10}^c from table 1) are shown for the two flashes. The values for the two flashes have been normalized to each other for the 2 – 2.5 Km altitude bin. A US-standard atmosphere (Group, 1976) is used to relate pressure and altitude.

pressure halves. Since the radiated power is expected to be proportional to the current-change, we thus expect the radiated power to decrease strongly with increasing height like is shown from our results. However, the strong increase of pulse strength towards lower altitudes appears not consistent with the laboratory results and rather suggest that the proximity of the ground plays is important.

Another interesting observation is that the amplitude distributions at the highest amplitudes (where imaging efficiency is constant) shows an approximately linear dependency on a double log-scale. This strongly implies that the amplitude distribution follows a power law, which is scale invariant. The values for this power, as shown in table 1, vary considerably, probably due to poor statistics, but seem to have a mean value of about 3. No distinct height dependence is shown by the results. In a future work we will investigate this in more detail. The pulse distribution should reflect the distribution of streamer intensities in a corona flash. In the literature we could, unfortunately, not find predictions for the distribution of streamer intensities in a corona flash.

Acknowledgments

This study was financed in part by the Coordenação de Aperfeiçoamento de Pessoal de Nível Superior – Brasil (CAPES) – Finance Code 001 and by the Fundação de Apoio à Pesquisa do Distrito Federal - FAP/DF. The LOFAR cosmic-ray key science project acknowledges funding from an Advanced Grant of the European Research Council (FP/2007-2013) / ERC Grant Agreement n. 227610. The project has also received funding from the European Research Council (ERC) under the European Union's Horizon 2020 research and innovation programme (grant agreement No 640130). We furthermore acknowledge financial support from FOM, (FOM-project 12PR304). ST acknowledges funding from the Khalifa University Startup grant (project code 8474000237). BMH is supported

by NWO (VI.VENI.192.071). KM is supported by FWO (FWO-12ZD920N). AN acknowledges the DFG grant NE 2031/2-1. TNGT acknowledges funding from the Vietnam National Foundation for Science and Technology Development (NAFOSTED) under [Grant number 103.01-2019.378]. LOFAR, the Low Frequency Array designed and constructed by ASTRON, has facilities in several countries, that are owned by various parties (each with their own funding sources), and that are collectively operated by the International LOFAR Telescope foundation under a joint scientific policy.

The data are available from the LOFAR Long Term Archive (for access see (ASTRON, 2020)). To download this data, please create an account and follow the instructions for "Staging Transient Buffer Board data" at (ASTRON, 2020). In particular, the utility "wget" should be used as follows:

`wget https://lofar-download.grid.surfsara.nl/lofigrid/SRMFifoGet.py?surl="location"`

where "location" should be specified as:

`srm://srm.grid.sara.nl/pnfs/grid.sara.nl/data/lofar/ops/TBB/lightning/` followed by

`L612746\_D20170929T202255.000Z_"stat"_R000_tbb.h5` (for the 2017 Flash),
`D20180813T153001.413Z_"stat"_R000_tbb.h5` (for the 2018 Flash),

and where "stat" should be replaced by the name of the station, CS001, CS002, CS003, CS004, CS005, CS006, CS007, CS011, CS013, CS017, CS021, CS024, CS026, CS028, CS030, CS031, CS032, CS101, CS103, RS106, CS201, RS205, RS208, RS210, CS301, CS302, RS305, RS306, RS307, RS310, CS401, RS406, RS407, RS409, CS501, RS503, RS508, or RS509.

References

ASTRON. (2020). *LOFAR Long Term Archive Access.* `https://www.astron.nl/lofarwiki/doku.php?id=public:lta_howto`.

Group, C. W. (1976). *U.s. standard atmosphere 1976,* (Tech. Rep. No. NASA-TM-X-74335). Washington, D.C.. Retrieved from `https://ntrs.nasa.gov/api/citations/19770009539/downloads/19770009539.pdf?attachment=true`

Hare, B. M., et al. (2019). Needle-like structures discovered on positively charged lightning branches. *Nature*, *568*, 360–363. doi: 10.1038/s41586-019-1086-6

Hare, B. M., Scholten, O., Dwyer, J., Ebert, U., Nijdam, S., Bonardi, A., et al. (2020). Radio emission reveals inner meter-scale structure of negative lightning leader steps. *Phys. Rev. Lett.*, *124*, 105101. Retrieved from `https://link.aps.org/doi/10.1103/PhysRevLett.124.105101` doi: 10.1103/PhysRevLett.124.105101

Li, X., Cui, X., Lu, T., Li, D., Chen, B., & Fu, Y. (2016). Influence of air pressure on the detailed characteristics of corona current pulse due to positive corona discharge. *Physics of Plasmas*, *23*(12), 123516. doi: https://doi.org/10.1063/1.4971804

Mulrey, K., Bonardi, A., Buitink, S., Corstanje, A., Falcke, H., Hare, B., ... Winchen, T. (2019). Calibration of the lofar low-band antennas using the galaxy and a model of the signal chain. *Astroparticle Physics*, *111*, 1-11. Retrieved from `https://www.sciencedirect.com/science/article/pii/S0927650518302810` doi: https://doi.org/10.1016/j.astropartphys.2019.03.004

Nijdam, S., Teunissen, J., & Ebert, U. (2020). The physics of streamer discharge phenomena. *Plasma Sources Science and Technology*, *29*(10), 103001. Retrieved from `https://doi.org/10.1088/1361-6595/abaa05` doi: 10.1088/1361-6595/abaa05

Scholten, O., Hare, B. M., Dwyer, J., Sterpka, C., Kolmasova, I., Santolik, O., et al. (2021). The initial stage of cloud lightning imaged in high-resolution. *Journal of Geophysical Research: Atmospheres*, *126*(4), e2020JD033126. Retrieved

from https://agupubs.onlinelibrary.wiley.com/doi/abs/10.1029/2020JD033126 doi: https://doi.org/10.1029/2020JD033126

Shi, F., Liu, N., Dwyer, J. R., & Ihaddadene, K. M. A. (2019). Vhf and uhf electromagnetic radiation produced by streamers in lightning. *Geophysical Research Letters*, *46*(1), 443-451. Retrieved from https://agupubs.onlinelibrary.wiley.com/doi/abs/10.1029/2018GL080309 doi: https://doi.org/10.1029/2018GL080309

T, H., A.J.M., P., W.F.L.M., H., F.J.C.M., B., & E.J.M., v. H. (2013). Temperature and pressure effects on positive streamers in air. *Journal of Physics D*, *46*, 165202. doi: http://dx.doi.org/10.1088/0022-3727/46/16/165202

T.M.P, B., van Veldhuizen, E., & Ebert, U. (2008). Positive streamers in air and nitrogen of varying density: experiments on similarity laws. *Journal of Physics D*, *41*, 234008. doi: http://dx.doi.org/10.1088/0022-3727/41/23/234008

van Haarlem, M. P., et al. (2013). Lofar: The low-frequency array. *Astronomy & Astrophysics*, *556*(A2). doi: https://doi.org/10.1051/0004-6361/201220873